Phosphorylation regulates human polη stability and damage bypass throughout the cell cycle

Federica Bertoletti[1],[†], Valentina Cea[1],[†], Chih-Chao Liang[2], Taiba Lanati[1], Antonio Maffia[1],[3], Mario D.M. Avarello[1], Lina Cipolla[1], Alan R. Lehmann[4], Martin A. Cohn[2] and Simone Sabbioneda[1],*

[1]Istituto di Genetica Molecolare-CNR, 27100, Pavia, Italy, [2]Department of Biochemistry, University of Oxford, OX1 3QU, Oxford, UK, [3]Dipartimento di Biologia e Biotecnologie 'Lazzaro Spallanzani', Universita` degli Studi di Pavia, 27100, Pavia, Italy and [4]Genome Damage and Stability Centre, University of Sussex, BN1 9RQ, Brighton, UK

ABSTRACT

DNA translesion synthesis (TLS) is a crucial damage tolerance pathway that oversees the completion of DNA replication in the presence of DNA damage. TLS polymerases are capable of bypassing a distorted template but they are generally considered inaccurate and they need to be tightly regulated. We have previously shown that polη is phosphorylated on Serine 601 after DNA damage and we have demonstrated that this modification is important for efficient damage bypass. Here we report that polη is also phosphorylated by CDK2, in the absence of damage, in a cell cycle-dependent manner and we identify serine 687 as an important residue targeted by the kinase. We discover that phosphorylation on serine 687 regulates the stability of the polymerase during the cell cycle, allowing it to accumulate in late S and G2 when productive TLS is critical for cell survival. Furthermore, we show that alongside the phosphorylation of S601, the phosphorylation of S687 and S510, S512 and/or S514 are important for damage bypass and cell survival after UV irradiation. Taken together our results provide new insights into how cells can, at different times, modulate DNA TLS for improved cell survival.

INTRODUCTION

DNA replication is crucial for the perpetuation of genetic information. To ensure its completion, cells possess damage tolerance mechanisms that are capable of replicating a template even when DNA damage is present. One of such tolerance systems is DNA translesion synthesis (TLS) and it takes advantage of specialized DNA polymerases to allow the progression of the replication fork in the presence of a distorted template (1). The majority of TLS polymerases belong to the Y family and include polη, polι, polκ and Rev1 along with the B-family member polζ (1). The Y family polymerases can bypass the damage by virtue of a more open catalytic site that can accommodate DNA lesions, such as cyclobutane pyrimidine dimers (CPDs), created by exposure to UV light (2). As a trade-off, this wider catalytic site is prone to errors during nucleotide incorporation, so TLS polymerases need to be tightly controlled. This regulation is achieved in multiple ways in different model organisms: while in *Saccharomyces cerevisae* the concentration of TLS polymerases seems to be regulated (3), in mammalian cells TLS polymerases are believed to be regulated mainly by modulating their localization and recruitment to DNA (3). Post-translational modifications (PTMs) play a fundamental role in such control, and numerous lines of evidence now support the notion that ubiquitylation, SUMOylation and phosphorylation are crucial in activating and blocking TLS in different contexts (4–9). Polη is one of the main TLS polymerases and is the only one that can bypass CPDs in an error-free manner. The genetic disease, xeroderma pigmentosum variant, which is caused by inactivating mutations in the *POLH* gene, exemplifies its importance (10). Polη can be considered the archetypal TLS polymerase on the subject of PTMs as it has been shown to be ubiquitylated, phosphorylated and more recently SUMOylated (4–5,7,9,11–12). Polη is monoubiquitylated on one of four lysines present on its PCNA (proliferating cell nuclear antigen) interacting region (PIR) (4). This modification occurs in the absence of DNA damage and prevents the interaction of the polymerase with ubiquitylated targets that is mediated by its UBZ (ubiquitin binding zinc finger) motif. Once ubiquitylated, polη transitions to an inactive state via an intramolecular conformational change. This structural change allows the UBZ to make contact with the ubiquitin attached to the PIR, thus blocking it from binding to other ubiquitylated proteins. Monoubiquitylation has been shown to prevent polη from

*To whom correspondence should be addressed. Tel: +39 0382 546339; Fax: +39 0382 422286; Email: simone.sabbioneda@igm.cnr.it
†These authors contributed equally to the paper as first authors.

interacting with PCNA, the polymerase clamp, which plays a crucial role in controlling damage tolerance. The E3 ligases PirH2 and Mdm2 have been suggested to be responsible for this regulatory monoubiquitylation of polη and previously it has been shown to be linked to the proteasomal degradation of the polymerase (13–15).

While the ubiquitylation of polη appears to have an inhibitory effect on TLS, the phosphorylation of the polymerase leads to its full activation. After DNA damage polη is phosphorylated by the PI3 kinase Ataxia Telangiectasia and Rad3 related (ATR) on serine 601, and this modification is required for efficient damage bypass (5). Phosphorylation of S601 occurs only on chromatin and it requires polη UBZ and depends on Rad18 but not on PCNA ubiquitylation. In recent years it has been suggested that other polη residues might be phosphorylated but direct evidence of their modification is still missing (12).

Here we report that polη exists in multiple phosphorylation states even in the absence of DNA damage and its phosphorylation changes in a cell cycle-dependent manner. We identify novel phosphorylated sites and show that one of them (S687) affects polη protein stability.

MATERIALS AND METHODS

Cell culture and treatments

All the experiments in this study were carried out with SV40-transformed cells cultured in Dulbecco's modified Eagle's medium containing 10% Fetal Bovine Serum. XP30RO (XP-V, also designated GM3617) carries a homozygous deletion in the *POLH* gene, resulting in a truncated protein of 42 amino acids. The SV40-transformed cell line was originally established by Cleaver *et al*. (16). The absence of the polη protein was routinely monitored by immunoblotting and by UV sensitivity assays. MRC5V1 cells (also called MRC5) are SV40-transformed normal lung fibroblasts.

eGFP-tagged mutants of polη (S687A and SSSAAA) cloned in pEGFP-C3 were created by Quickchange site directed mutagenesis (Stratagene) using the following primers and verified by sequencing:

S687A: primer forward 5′-GCAAAAGAAATCCCAAG GCCCCTTTGGCCTGCAC-3′, primer reverse 5′-GTG CAGGCCAAAGGGGCCTTGGGATTTCTTTTGC-3′.

SSSAAA: primer forward 5′-CTCAGGCTCCCATGG CCAATGCCCCAGCCAAGCCCTCATTACC-3′, primer reverse 5′-GGTAATGAGGGCTTGGCTGGGGCATTG GCCATGGGAGCCTGAG-3′.

Once obtained, eGFPpolη and its mutants were subcloned in pCDNA3.1(+) (Thermo Scientific) by digestion with NheI and BamHI to obtain plasmids suitable for the TNT Quick coupled Transcription/Translation system (Promega).

XP30RO stably expressing S687A or SSSAAA were created using previously described procedures (5,17). Briefly 4×10^5 cells were seeded on a 6 cm dish and transfected (see below) with the relevant construct. After 24 h, the cells were diluted in four 10-cm dishes and selected in 1 μg/ml G418. Single colonies were collected after 14 days in culture with cloning discs (Sigma–Aldrich) and expanded. Finally

the clones were screened for the presence of eGFPpolη before enrichment with a cell sorter.

MG132 (Sigma–Aldrich) was used at 10 μM for 1, 3 or 6 h. Roscovitine (Selleckchem) was used at the final concentration of 20 μM for 1, 3 or 6 h. Dinaciclib (Selleckchem) was used at the final concentration of 100 nM for 2 or 8 h. VE-821 (Sellekchem) was used at 10 μM for 1 hour.

Cell synchronization was performed with a double thymidine (Sigma–Aldrich) block and a release in nocodazole (Sigma–Aldrich) if not otherwise stated. Cells were treated for 16 h with 2.5-mM thymidine, released in medium without thymidine and then incubated again for 16 h in thymidine. Finally, the cells were released into 50 ng/ml nocodazole for up to 16 h and were harvested at different time points. Transfection was carried out with Viafect (Promega) or Genejuice (Novagen) according to the manufacturers' instructions.

2D gel electrophoresis

All reagents and solutions for 2D-PAGE (polyacrylamide gel electrophoresis) were obtained from Bio-Rad except as noted. Cell pellets were resuspended in 100 μl of rehydration buffer with protease and phosphatase inhibitors and sonicated for 3 cycles/30 s with a Diagenode Bioruptor. Benzonase (50U) (Merk Millipore) was added and the extracts were incubated end over end for 30 min at 4°C. Samples were then centrifuged at 13 000 rpm for 30 min at 4°C and quantified by Bradford assay. A total of 120 μg protein extract were diluted with rehydration buffer to a final volume of 200 μl.

A total of 200 μl of each sample were loaded on a 7 cm IPG strip (pH3–10) by passive rehydration for 30 min followed by an active rehydration in a Bio-Rad Protean i12 IEF cell (14 h 50V 20°C).

The first dimension was performed at 50 mA on a voltage gradient. Following focusing, each strip was incubated for 20 min twice in equilibration buffer with 20 mg/ml dithiothreitol (DTT) or 25 mg/ml iodoacetamide (Sigma–Aldrich) respectively. Strips, embedded in agarose, were then loaded on 10% polyacrylamide gels.

Electrophoresis was performed at 100 mA for 10 min and then at a constant current of 200 mA for 60 min.

SDS-PAGE and western blotting

Proteins separated by sodium dodecyl sulphate-polyacrylamide gel electrophoresis (SDS-PAGE) were transferred onto nitrocellulose membranes. After blocking in 5% skim milk powder in Tris-buffered saline, pH 7.5, 0.1% Tween-20 for 1 h at room temperature, the membranes were incubated with primary antibodies overnight at 4°C. The membranes were then incubated with secondary antibody and visualized using an enhanced chemiluminescence detection kit (Millipore) on a LAS500 system (GE Healthcare). Western blots were analyzed with Imagequant (GE Healthcare).

Antibodies

Antibodies used in this study included: anti-mouse-BrdU (Becton Dickinson, 1:200); Vimentin (Sigma–Aldrich,

1:1000); Vinculin (Abcam, 1:1000); Phospho-CDK Substrate Motif [(K/H)pSP] (Cell Signaling 1:1000); Polη (Abcam, 1:1000, used only for detection of eGFPpolη); Polη (custom made 1:500, detects endogenous polη); Polη P-687 (custom made, 1:200); PCNA (Santa Cruz, 1:1000).

RNA extraction, RT-PCR and real-time PCR

Total RNA was extracted using a Qiagen RNA Kit according to the manufacturer's instructions. One microgram of total RNA was used for cDNA synthesis with a M-MulV Reverse Transcriptase Kit (Roche). Amplification conditions were as follows: 60 min at 37°C followed by 10 min at 70°C. Real-time polymerase chain reaction (PCR) was performed using iTaq™ Universal SYBR® Green Supermix (Bio-Rad) in a LightCycler 480 (Roche). Reactions were run in triplicate in three independent experiments. The housekeeping gene used was GAPDH.

The primers used are:

GAPDH: primer forward 5′-ACCACAGTCCATGCCATCAC-3′ primer reverse 5′-TCCACCACCCTGTTGCTGTA-3′.

Polη: primer forward 5′-AGTTCGTGAGTCCCGTGGG-3′ primer reverse 5′-GCTTGGCAACAAGTCTGCC-3′.

Clonogenic assay

Cell lines expressing different eGFP constructs were seeded and UV irradiated the following day at the indicated doses. After 13 days, the number of colonies was assessed after 70% EtOH fixation and methylene blue staining (0.1% Page-Blue; 50% MetOH; 7.5% Acid Acetic).

Post-replication repair (PRR) assay

Cells were washed in phosphate-buffered saline (PBS) and irradiated with 8 Jm^{-2} as previously described [4]. Briefly, cells were incubated in 2 ml of medium containing 0.3 mg/ml caffeine for 30 min before the addition of 1.85 MBq of ^{3}H-thymidine. Cells were then released in fresh caffeine-containing medium (0.3 mg/ml) supplemented with 10 μM thymidine and 10 μM deoxycytidine for 150 min. At the end of the chase period, cells were collected in PBS containing ethylenediaminetetraacetic acid (EDTA) (0.2 g/l). Cells were then lysed in 0.2 ml buffer (1% SDS, 0.75M NaOH, 0.75M NaCl, 20 mM EDTA) layered on top of 5 ml of a 5–20% sucrose gradient (in 0.1 M NaOH, 0.1 M NaCl). After exposure to visible light for 1 h, the gradients were spun at 38 500 rpm for 70 min in a Sw55 rotor. At the end of the run, 25 fractions were spotted on Whatman grade 17 paper, precipitated by trichloracetic acid and washed twice in ethanol before being counted on a Perkin Elmer scintillation counter. The weight-average molecular weights of the distributions were calculated as [18], omitting the top and bottom three fractions.

Flow Cytometry analysis

Cells were harvested after incubation with 30 μM bromodeoxyuridine (BrdU; Sigma–Aldrich) for 30 min, fixed in 1 ml of cold 70% ethanol and stored at 4°C. DNA was denatured with 2N HCl and 0.5% Triton X-100, then neutralized with 1 ml of 0.1M sodium borate pH8.5. The cell pellet was resuspended in PBS, 0.5% Tween 20, 1% bovine serum albumin (BSA) with a mouse anti-BrdU antibody (Becton Dickinson, Franklin Lakes, NJ, USA) and incubated at room temperature for 1 h, followed by 1-h room temperature incubation with anti-mouse-488 (Alexa anti-mouse 488, Molecular Probes/Invitrogen). Samples were finally incubated with 10 μg/ml Propidium Iodide and analyzed on a S3 flow cytometer (Biorad). Data were analyzed using the program ProSort (Biorad) or FCS Express (DeNovo). When Propidium Iodide only staining was performed, cells were fixed in 1 ml of cold ethanol and resuspended in PBS, 0.1% Tween 20, 50 μg/ml Propidium Iodide, 5 μg/ml RNase A. After incubation at 37°C for 15 min, cells were analyzed by flow cytometry.

In vitro CDK assay

Assays for polη phosphorylation were performed with CDK1 and CDK2. The reactions were performed with the same units of enzymes (10U) or with the same quantity of enzymes (40 ng). Purified polη was incubated either with CDK1/cyclin B (Millipore) or CDK2/cyclin A (Millipore) in reaction buffer (8 mM MOPS/NaOH pH7.0, 2.5 mM MgAc, 0.05 mM ATP, 0.02 mM EDTA) for 10 min at 30°C. The reactions were stopped by addition of Laemmli buffer and boiled at 95°C for 5 min. Activity of the CDKs was checked by incubating the kinases with Histone H1 (Sigma–Aldrich).

Immunoprecipitation

Harvested cells were lysed with a lysis buffer (0.5% NP40, 40 mM NaCl, 50 mM Tris–HCl pH 7.5, 2 mM MgCl$_2$, 1 mM N-Ethylmaleimide (NEM), protease inhibitors cocktail (Roche), phosphatase inhibitors (Roche) and 1 μl/ml Benzonase (Novagen)) and incubated on a rotary wheel at 4°C for 30 min. After incubation the mixture was centrifuged at 13 000 rpm for 15 min at 4°C and the supernatants were collected and quantified by Bradford assay. Samples were diluted in four volumes of immunoprecipitation (IP) buffer (125 mM NaCl, 50 mM Tris–HCl pH 7.5, protease inhibitors cocktail (Roche)). Protein extracts were pre-cleared with Protein A/G magnetic beads (100 μl/20 mg of protein, Thermo Scientific), previously equilibrated with three volumes of IP buffer, before IP with anti-GFP antibody (Thermo Scientific) bound to protein A/G magnetic beads.

Protein purification and MS analysis

Polη−6His, was purified from *Escherichia coli* as previously described [19]. GST-PCNA was bought from Thermo Fisher Scientific. Flag-HA Polη was purified and analyzed by liquid chromatography-tandem mass spectrometry (MS) as described in [20].

Phosphatase treatment

A total of 120 μg protein extracts were incubated in phosphatase buffer (New England Biolabs) with or without

1600U of λ phosphatase (New England Biolabs) for 30 min at 30°C. After incubation the reaction was diluted with rehydration buffer up to a volume of 200 μl and processed as previously described for 2D-PAGE. Alternatively, immunoprecipitated proteins were incubated with 800U of λ phosphatase for 1 h in phosphatase buffer at 30°C before resuspension in Laemmli buffer.

Primer extension assay

Plasmids encoding eGFPpolη (WT, S687A and SSSAAA) or polη-6His (WT and S687A) were used for *in vitro* coupled transcription and translation reactions in rabbit reticulocyte lysate according to manufacturer's instructions (Promega). Polymerases were quantified by western blot analysis and equimolar amounts of proteins were used for the primer extension assays. A 5′ FAM-labeled 13mer (5′ GGGTGGAGGTGAC 3′) was annealed with a template 33mer primer (5′ TCACACTCTATCACACTC[cis-syn-TT]GTCACCTCCACCC 3′) containing a thymidine dimer (TT) at position +14 (TriLink Biotechnologies). Primer extension assays were performed in 10 μl of replication buffer (40 mM Tris–Cl pH 8, 5 mM MgCl$_2$, 10 mM DTT, 0.25 mg/ml acetylated BSA, 60 mM KCl, 2.5% glycerol). Reactions were incubated at 37°C for 15 min and stopped with 10 μl of 2× loading buffer, (98% deionized formamide, 10 mM EDTA pH 8, 0.025% xylene cyanol and 0.025% bromophenol blue). Samples were boiled at 95°C for 5 min and rapidly chilled on ice. Reaction products were resolved on a 15% acrylamide-7M urea gel and then imaged on a Typhoon imager (GE HealthCare).

RESULTS

Polη presents multiple phosphorylation states

We previously identified and characterized S601 of polη and discovered how its phosphorylation was crucial for efficient damage bypass (5). The visualization of the phosphorylated state of the polymerase was extremely challenging and we had to develop a phospho-specific antibody in order to characterize the function of serine 601. In order to be able to assess the general phosphorylation state of the polymerase we adapted a new approach based on 2D SDS-PAGE. This technique relies on a first dimension that separates the proteins according to their isoelectric point followed by second dimension under denaturing conditions. This technique allowed us to amplify the small mobility shift caused by the polymerase phosphorylation as observed by canonical SDS-PAGE. We were surprised to note that polη separated in a number of different isoforms (Figure 1A) indicating that the polymerase could be modified by multiple phosphorylation events. To confirm that the different isoforms we were visualizing were indeed due to phosphorylation, we treated the cell extracts with λ−phosphatase. In such conditions all the negatively charged forms of polη disappeared indicating that our experimental approach had revealed multiple phosphorylated forms of the polymerase (Figure 1A). This finding was unexpected, as polη was previously shown to be phosphorylated only after DNA damage in order to trigger damage bypass (5). The damage-dependent phosphorylation of polη was carried out by the

ATR kinase. By exploiting our experimental set-up we confirmed that while polη is significantly phosphorylated in the absence of DNA damage, after UV exposure its phosphorylation profile changes toward a more acidic state (Figure 1B and C) and we confirmed that this hyper-phosphorylation was dependent on ATR as it could be abrogated by the ATR-specific inhibitor VE821 (Figure 1B and C).

Polη is phosphorylated during an unperturbed cell cycle

We wondered if the presence of multiple phosphorylation states in the absence of DNA damage could have functional significance in the regulation of the activity of the polymerase. In order to assess if the phosphorylation changed during the cell cycle, we synchronized the cells in early S phase via a double thymidine block and then released the cells. This allowed us to sample the global phosphorylation status of the polymerase at different stages of the cell cycle, notably during S phase, during anaphase transition and finally in the G1 of the next cell cycle phase. As can be seen in Figure 2A and B the phosphorylation of polη increases toward the end of the S phase before reaching a maximum when the cells are arrested at the -metaphase-anaphase transition because of the treatment with nocodazole. Once the cells reach the G1 phase of the following cell cycle, the phosphorylation profile reverts to a more basic state, indicating that the phosphorylation of polη is cell cycle regulated and is low in G1 before increasing in late S-G2. A BrdU incorporation assay confirmed that the cells progressed synchronously (Figure 2C). The cell cycle-dependent phosphorylation of polη occurred also when the cells were released in the absence of nocodazole, indicating that the progression through the cell cycle was responsible for the modification and not the treatment with the drug (Supplementary Figure S1A).

CDKs are responsible for the cell cycle phosphorylation of polη

Given the peculiar distribution of polη phosphorylation through the cell cycle, we investigated if the polymerase could be the target of CDKs. To address this hypothesis we synchronized the cells in mitosis with nocodazole. In this condition, the phosphorylation of polη is maximal, with an evident shift toward an acidic isoelectric point (compare Figure 3A/B first and second blot). After treatment with nocodazole, the cells were further treated with two CDK inhibitors, specifically roscovitine and Dinaciclib. Both are known to be capable of repressing the activity of various CDKs (21,22). In both cases we detected a shift in the mobility of polη, consistent with a reduction in phosphorylated forms (compare third and fourth blot with the second in Figure 3A/B). Overall polη was unphosphorylated in roscovitine and Dinaciclib-treated cells, indicating that CDKs played a major role in regulating the cell cycle-dependent phosphorylation of the polymerase. The change in polη phosphorylation after CDK inhibition was also detectable in cycling cells without nocodazole arrest (Supplementary Figure S1B), indicating that the observed phenomenon was not due to the synchronization protocol. Although the phosphorylation was significantly reduced by
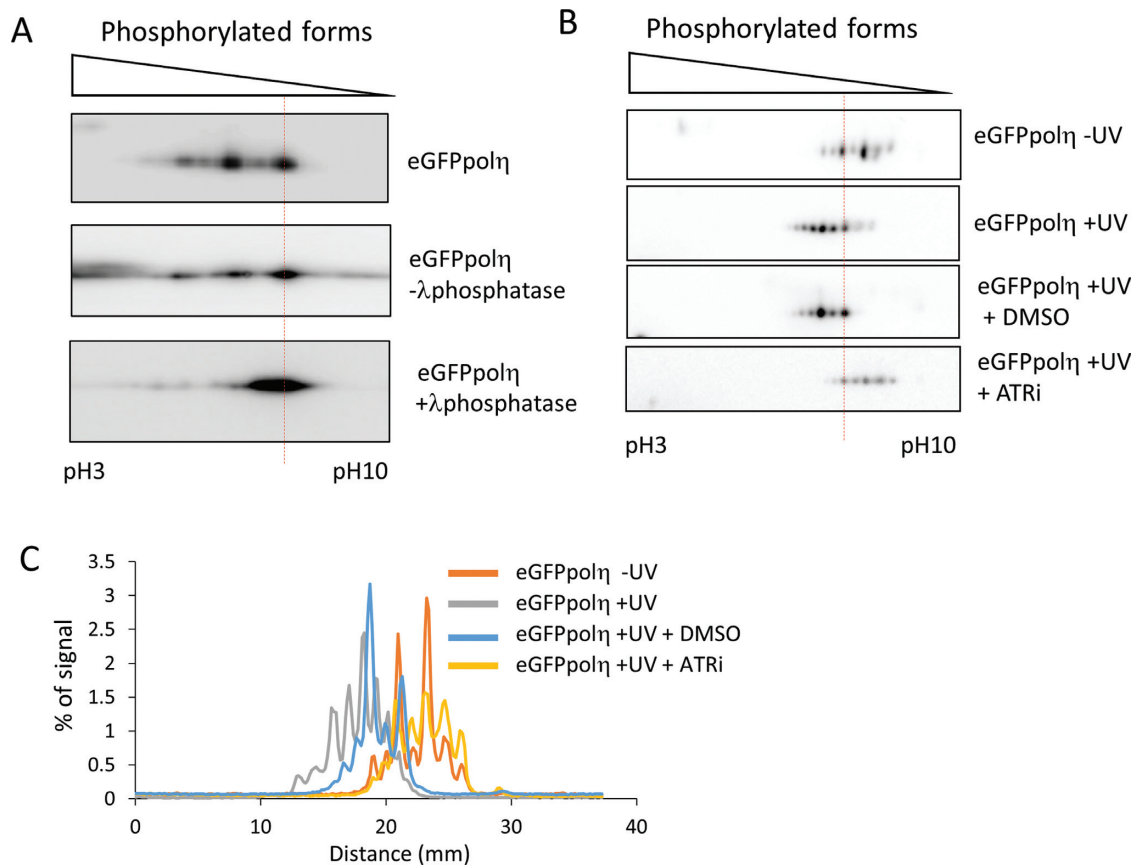
Figure 1. DNA polymerase η is phosphorylated even in the absence of DNA damage. (**A**) 2D-PAGE analysis of XP30RO cells expressing eGFPpolη shows the protein separating at different isoelectric points. Top blot, cell extract processed before incubation with phosphatase buffer. Middle blot, cell extract after incubation in phosphatase buffer at 30°C for 30 min. Bottom blot, cell extract after incubation with λ-phosphatase in phosphatase buffer at 30°C for 30 min. The different isoforms disappear after treatment with λ-phosphatase indicating that they represent phosphorylated forms of the polymerase. The 2D PAGE were aligned by using Vimentin and PCNA as triangulation markers (see Figure 2). The red dotted line is used as reference of the alignment. (**B**) DNA polymerase η becomes hyper-phosphorylated after damage in an ATR-dependent manner. (**C**) Densitometric analysis of the blots presented in B.

the treatments, some modified form of polη persisted, indicating that either redundant CDKs are involved or other kinases could phosphorylate polη.

At this point, we could only conclude that CDKs were important in regulating the phosphorylation of polη, but we did not know if they directly phosphorylated polη or if the phosphorylation was mediated by one of the plethora of CDK substrates. To address this point we purified human polη and performed an *in vitro* kinase assay. CDK2 and CDK1 are the two major kinases involved in S phase and G2/M phase progression. For this reason we chose to test their kinase activity using polη as substrate. Equal units of CDK1/2 or equal amounts (ng) of active kinases (Supplementary Figure S2A) were incubated with polη before electrophoresis. In order to monitor the phosphorylation activity, we used an antibody able to recognize phosphorylated CDK targets at their consensus motif ((K/R)(S*)PX(K/R)). As can be seen in Figure 3C, polη was efficiently phosphorylated by CDK2 but hardly by CDK1. We therefore concluded that polη was phosphorylated directly by CDK2 in a cell cycle-dependent manner.

Identification of new polη phosphorylation sites

To try to identify the specific residues that were phosphorylated, Flag-HA-tagged polη (e-Polη) was stably expressed in HeLa cells. e-Polη was purified, excised from an SDS-PAGE gel (Figure 4A) and analyzed by MS/MS, leading to the identification of new putative phosphopeptides. The MS analysis confidently assigned a phosphorylation on S687 (Figure 4B, top panel), and another single phosphate on a peptide containing S510, S512, S514 (Figure 4B, bottom panel). In this case, it was not possible to pinpoint exactly which of the three closely clustered serines was modified. As can be seen in Figure 4C, the new phosphorylation sites lie toward the C-terminus of the polymerase with S510, S512, S514 located right after the catalytic domain while S687 resides in the Nuclear Localization Signal (NLS).

To verify that the phosphorylated peptides identified in the MS analysis were indeed phosphorylated, we established a series of XP30RO cell lines stably expressing alleles of the polymerases that were mutated at S687 and S510, S512, S514 (SSSAAA). All the alleles were tagged with eGFP, as we have previously shown that this tag did not
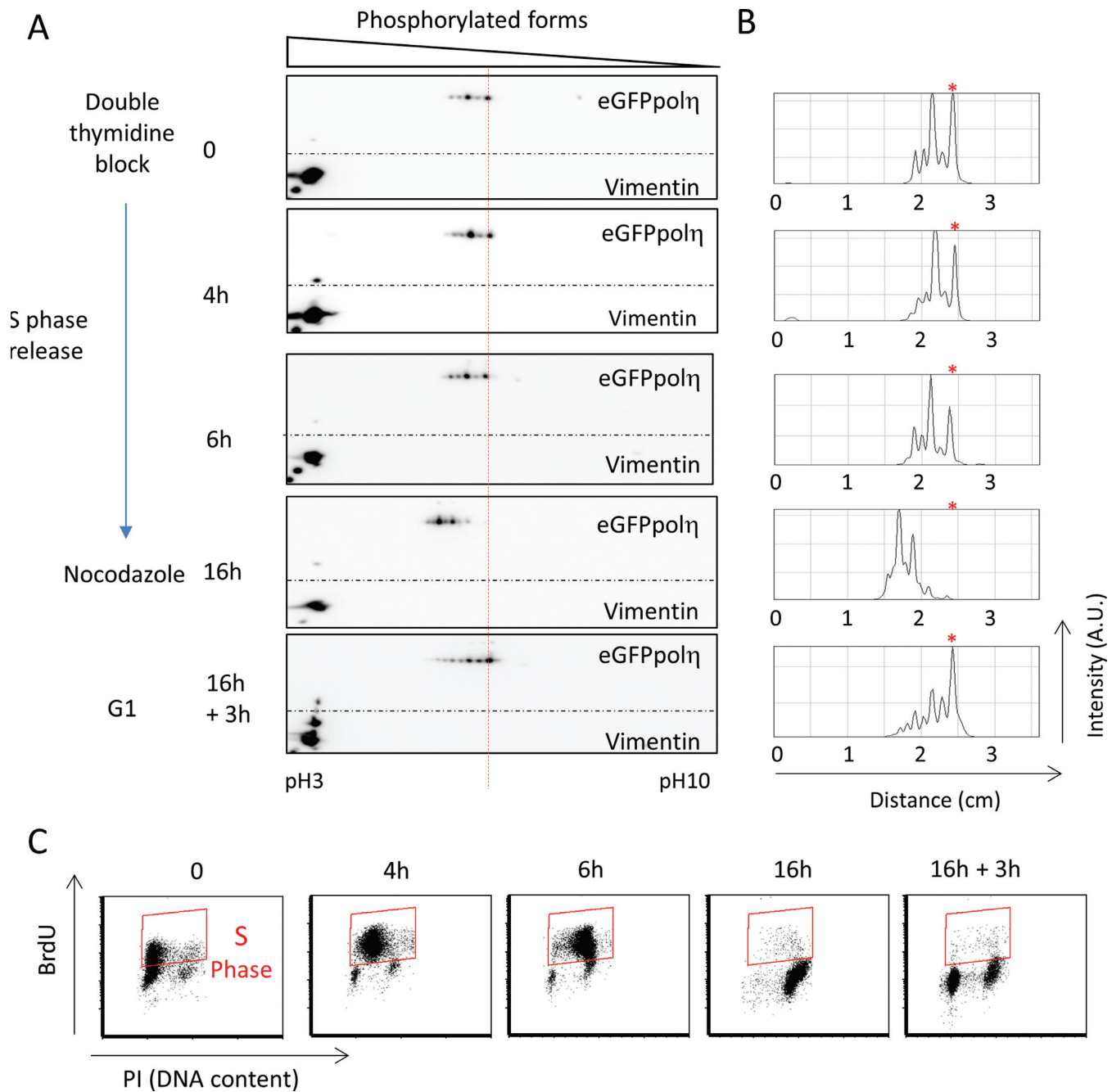
Figure 2. DNA polymerase η phosphorylation changes during an unperturbed cell cycle. XP30RO cells expressing eGFPpolη were synchronized by double thymidine block (0) before being released into S phase in the presence of nocodazole. After 16 h, the cells arrested in anaphase and they were subsequently released into the G1 phase of the next cell cycle (16 + 3). 2D-PAGE shows increasing amounts of phosphorylated polη during the transition from S to G2/M before a reduction in G1. The dotted line is used as reference of the alignment. (**B**) Densitometric analysis of the blots presented in A, the asterisk marks the reference peak as in A. (**C**) BrdU analysis of the experiment shown in panel A shows a synchronized progression through the cell cycle.

interfere with the protein catalytic activity (Supplementary Figure S3A), localization or function (4,17,23). We then performed a 2D-PAGE analysis to assess the phosphorylation pattern of the mutants. As can be seen in Figure 4D, both S687A and SSSAAA showed a marked reduction in the number of phosphorylated species, going from seven in the WT to four in each mutant.

Mutations in either of these residues did not completely abolish the phosphorylation of polη, indicating that S687

and S510, S512, S514 are phosphorylated independently and other phosphorylated forms of the polymerase are still present. Furthermore, the isoelectric point of the polymerase changed, with a new more basic spot appearing in the mutants. This could indicate that in the WT all of the polymerase is phosphorylated and the unphosphorylated form becomes evident only when some of the phospho-sites are mutated or the CDKs are inhibited (See Dinaciclib blot in Figure 3A and B).
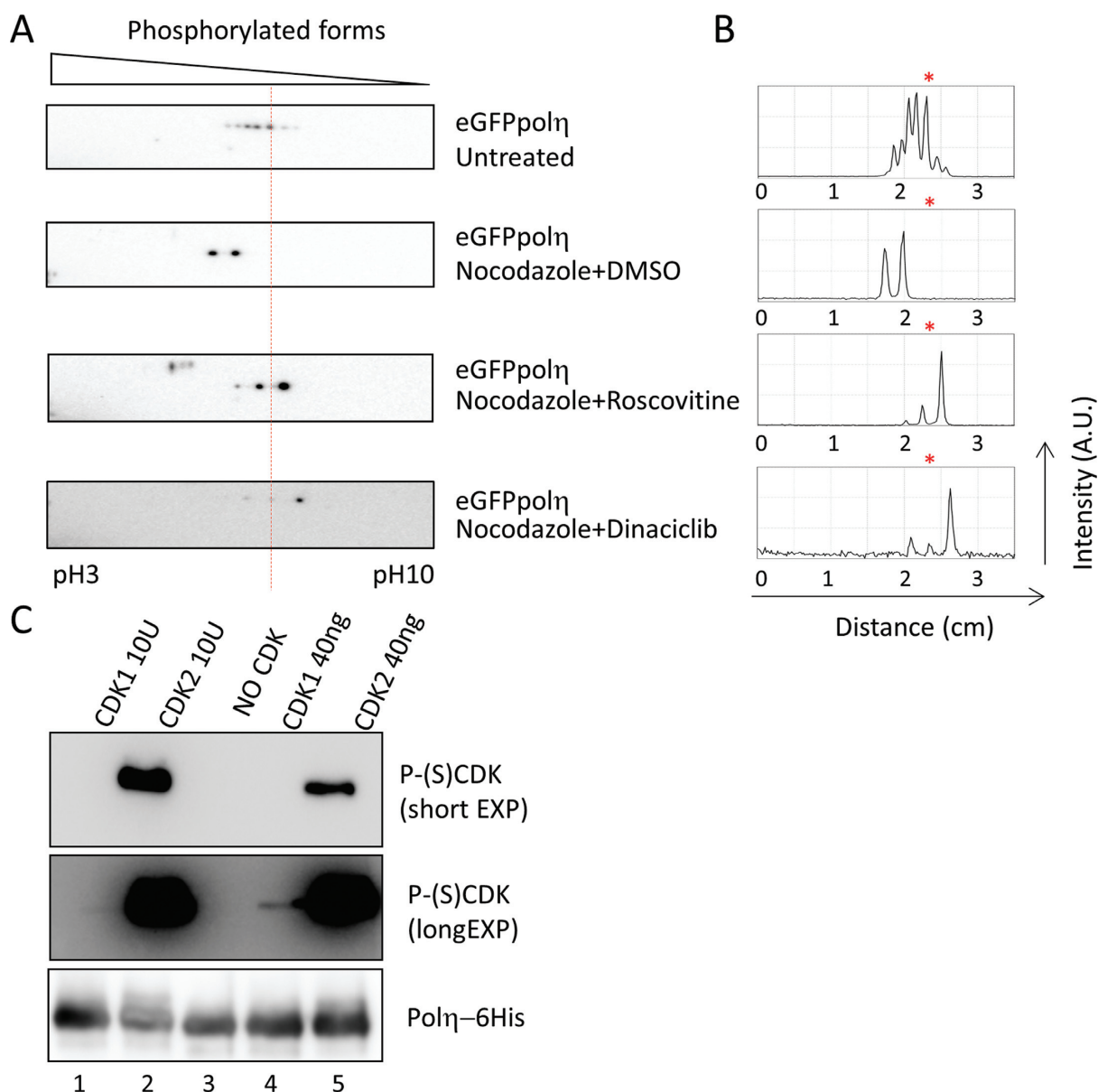
Figure 3. DNA polymerase η phosphorylation is dependent on CDKs. XP30RO cells expressing eGFPpolη were synchronized in anaphase by nocodazole before treatment with CDK inhibitors. (**A**) 2D-PAGE analysis of polη shows a reduction of phosphorylated forms after treatment with two pan CDK inhibitors (Dinaciclib and roscovitine). Gels were aligned by using Vimentin (shown) and PCNA (not shown) as first dimension migration markers. (**B**) Densitometric analysis of the blots presented in A, the asterisk marks the peak used as reference. (**C**) *In vitro* kinase assay with purified polη and purified CDK1 or CDK2.

Up to this point, we could successfully monitor the global phosphorylation status of polη, without being able to discern specifically the behavior of a specific residue. To overcome this limitation, we developed a phospho-specific antibody raised against P-S687. Unfortunately, we could not establish an antibody against the other residues due to the difficulty in pinpointing which serine was modified. The new antibody was able to detect phosphorylated polη specifically on S687 as can be seen in Figure 4E. We also verified that the signal was due to a phosphorylation modification as a signal was absent when polη was immunoprecipitated and treated with λ-phosphatase (Supplementary Figure S2, compare lanes 3 and 4 with 9 and 10). The development of

this antibody gave us the opportunity to specifically study this modification *in vivo*.

S687 is a CDK target and is regulated during the cell cycle

As shown before, the phosphorylation of polη was affected by CDK inhibitors *in vivo* and was a direct target of CDK2 *in vitro*. The identification of new putative phosphorylated residues prompted us to examine if S687 and S510, S512, S514 were CDK targets *in vivo*. After IP, we were not able to detect a signal from the CDK phospho-specific antibodies when S687A was expressed, while it was unchanged in the SSSAAA mutant (Figure 5). This suggested that only S687 was a target of CDKs *in vivo*. It should also be noted
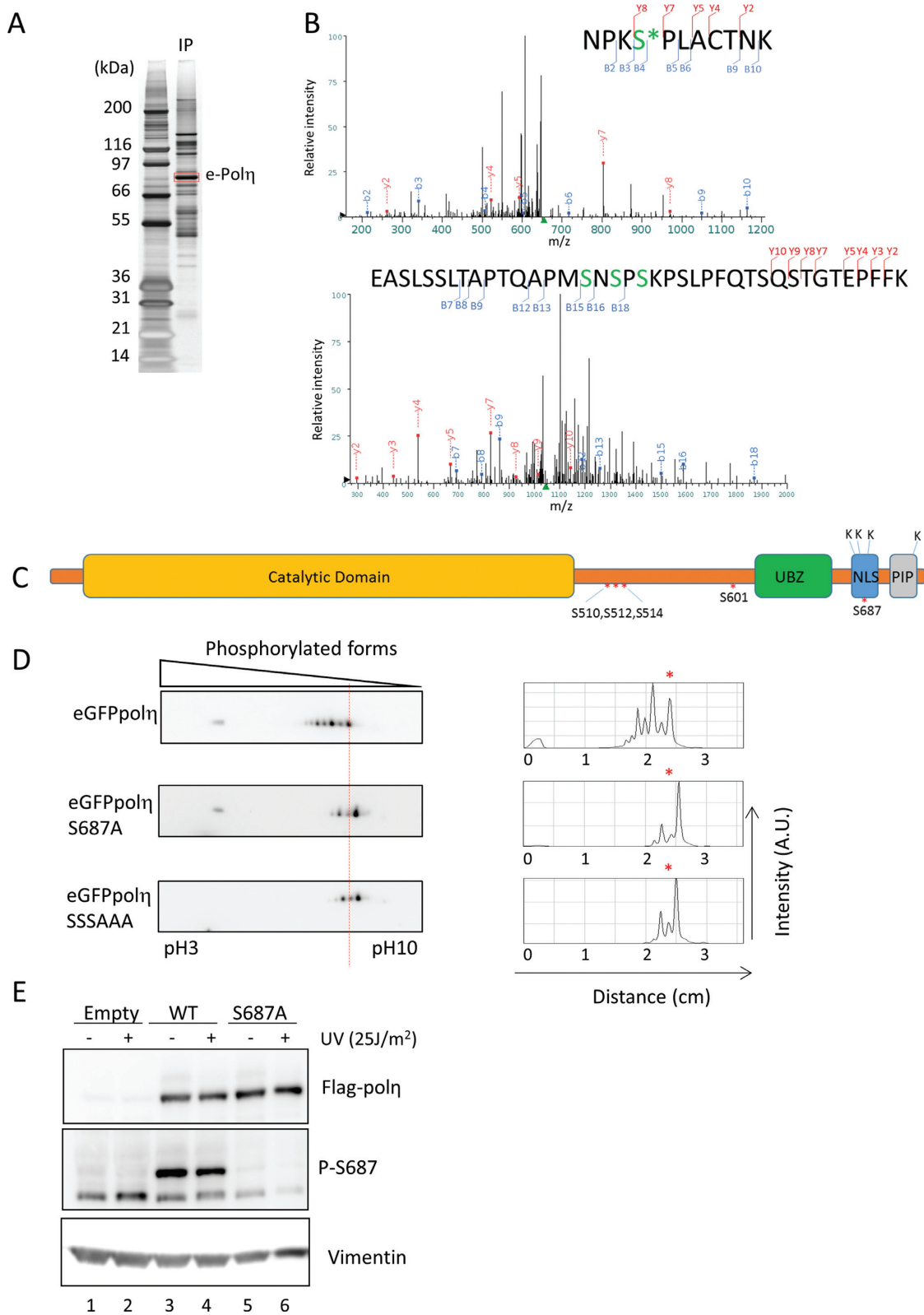
Figure 4. Identification of new phosphorylated residues in Polη. (**A**) e-Polη was purified and extracted from the gel for MS/MS analysis. (**B**) MS/MS spectra of the new phosphorylation sites of polη. B ions are marked in blue and Y ions are marked in red, both in the spectra and the peptide sequences. The top spectrum represents the peptide containing P-S687 (*site confidently assigned) while the bottom spectrum represents a peptide (aa 495–533) containing a single phosphate that could not be confidently assigned. Based on the fragmentation pattern the possible location of the phosphate was narrowed down to S510, S512 or S514. (**C**) Schematic representation of polη domains and alignment of newly identified phospho-residues. (**D**) 2D-PAGE analysis of XP30RO cells expressing eGFPpolη carrying S687A or S510A, S512A, S514A allele with respective densitometric analysis. The two mutant alleles show a reduced phosphorylation pattern. (**E**) Characterization of a new antibody against P-S687. Cells were transfected with Flag-polη either WT or S687A and probed with this antibody. Signal is present only in the case of the WT allele.
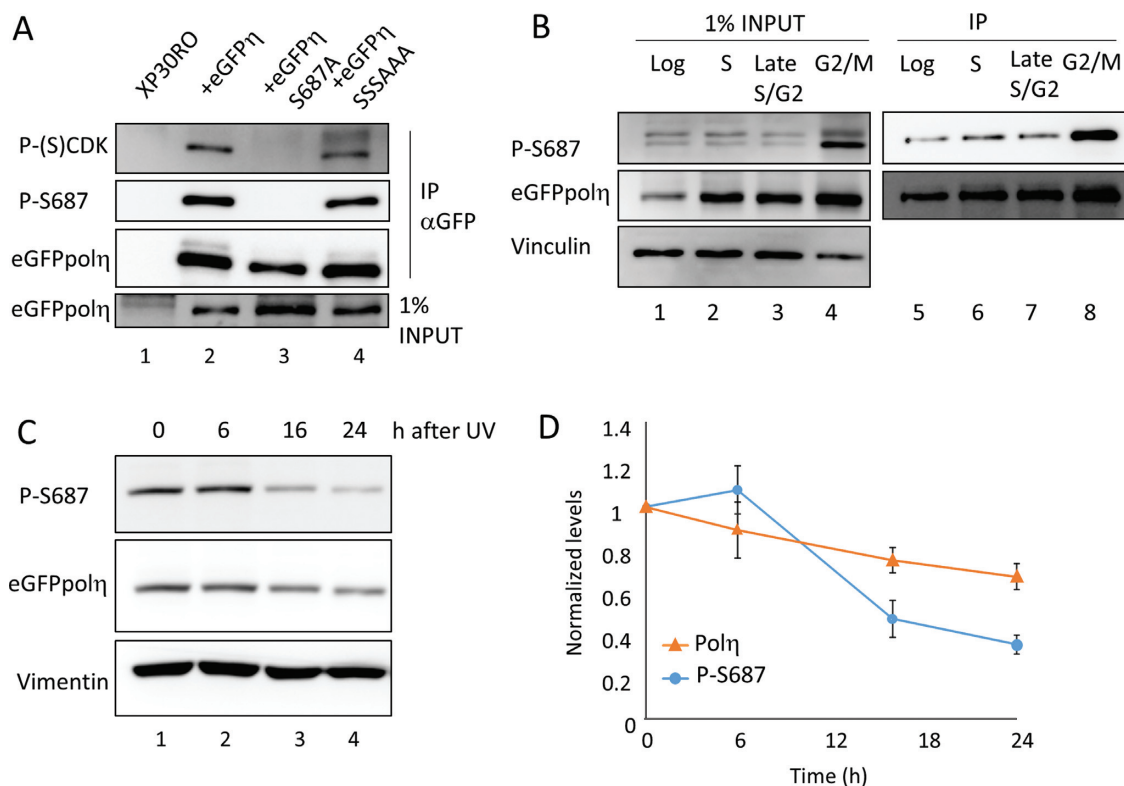
Figure 5. Serine 687 is phosphorylated by CDK and changes during the cell cycle and after UV irradiation. (**A**) eGFPpolη either WT, S687A or SSSAAA was immunoprecipitated from XP30RO derived cell lines and its phosphorylation status was analyzed with antibodies to P-(S)CDK and pS687. (**B**) XP30RO cells expressing eGFPpolη were synchronized by double thymidine block and released into the cell cycle in the presence of nocodazole, before IP of eGFPpolη. Polη and P-S687A increase in S phase and G2/M. (**C**) MRC5 cells were transfected with eGFPpolη and irradiated with 25 J/m^2 and followed for the indicated times. (**D**) Densitometric analysis of polη and P-S687 after UV irradiation. The signal of P-S687 was corrected for the levels of total polη. The plots represent the mean of three experiment ±S.E.M.

that the two phosphorylated regions are independently regulated as S687 is still phosphorylated in the SSSAAA mutant, indicating that the putative phosphorylation of S510, S512, S514 is not a prerequisite for the modification of S687 (Figure 5A, compare lane 2 with lane 4).

The phosphorylation of polη analyzed by 2D PAGE appeared to follow the progression of the cell cycle. To assess if S687 followed the same pattern and accounted for a part of the global cell cycle phosphorylation of polη we used the phospho-specific antibody to analyze polη in a single cell cycle after double thymidine synchronization. As can be seen in Figure 5B, phosphorylation of S687 peaks at the G2/M transition, with an 8-fold increase compared to the log phase sample, in a manner compatible with our previous observation (Figure 2A). Interestingly, we also detected a change in polη protein levels, with the polymerase being more abundant in S phase and G2/M than in the cells in log phase, where the G1 phase is more prominent.

As previously stated, polη is phosphorylated on S601 mainly after DNA damage. This holds true for both UV irradiation but also other DNA damaging treatments (5). In contrast, phosphorylation of S687 is detectable even in the absence of DNA damage and for this reason we speculated that it might be controlled in a different manner. To test the kinetics of phosphorylation of S687 after genotoxic insult we treated the cells with UV-C light and monitored

the presence of P-S687 over time. In contrast to what was recently reported (11) while this paper was in preparation, P-S687 levels did not increase after damage but slowly diminished, being halved 24 h after irradiation (Figure 5C and D). This suggested a marked difference from P-S601. Interestingly the level of polη itself also changed slightly (Figure 5C and D) after UV damage in accordance with what was previously observed in *Caenorhabditis elegans* (8,24). It is important to mention that the signal of P-S687 shown in Figure 5D was corrected for the levels of total polη, so the decrease in phosphorylation could not be explained simply by the reduction in the total amount of the polymerase.

The phosphorylation sites are important for damage bypass and cell survival

To test the effect of the different newly discovered phosphorylated residues on TLS, we used a series of XP30RO cells stably expressing different alleles of polη. The cell lines expressed eGFPpolη WT, S601A, S687A and SSSAAA. The cells were then sorted to perform the experiments with cells expressing polη at the same, near physiological, level. To assess for TLS proficiency, we monitored the cells in a clonogenic survival assay after increasing doses of UV. XP30RO cells are extremely sensitive to UV irradiation followed by incubation in the presence of caffeine and this has been

used as a diagnostic assay for a number of years. As can be seen in Figure 6A, expression of WT eGFPpolη rescued the UV sensitivity. Consistent with our previous report (5) the S601A mutant shows a lower survival than WT polη. Mutating S687 to alanine resulted in similar sensitivity and the survival rates of S601A and S687A are nearly identical. The triple S510512514A mutant appears to show a milder phenotype, although rescue of the sensitivity to the WT level was not complete. It is important to note that neither the S601A nor the SSS mutant affected the levels of phosphorylation at S687, as can be seen in Supplementary Figure S2C, and the signal disappeared only when serine 687 was mutated to alanine. Conversely, the phosphorylation of S601 was not affected in the S687A and SSS mutants suggesting that phosphorylation of S687 and P-S601 are indeed independent events.

To complement this analysis we examined also the post-replicative repair activity of the different mutants by following the size of nascent DNA in the presence of DNA damage. UV irradiated cells were pulsed with 3H-thymidine to label newly replicated DNA, before being chased further without the radioactive nucleoside. The size of newly synthesized DNA was then determined by running the DNA on an alkaline sucrose gradient. XP30RO cells cannot bypass the damage hence the DNA is replicated in shorter fragments (right side of the plot in Figure 6B). Complementation of XP30RO with WT polη rescues this deficiency and the cells are able to bypass the damage, resulting in DNA of larger size (left side of the plot in Figure 6B). All the mutants analyzed showed an intermediate phenotype, indicating that the damage bypass was impaired, ultimately resulting in UV sensitivity as shown by the clonogenic survival. Note that the catalytic activity of polη is unaffected in these mutants. It remained comparable between all our polη constructs, as monitored by *in vitro* primer extension assays (Supplementary Figure S3A).

Polη phosphorylation controls protein stability

While performing 2D-PAGE experiments we noticed that the treatment with roscovitine made the visualization of polη difficult. This required longer exposures for detection of the polymerase by western blot. Initially we linked this phenomenon to a decrease in protein expression after treatment with the CDK inhibitor. Roscovitine, by inhibiting the phosphorylation of RNApolII, is known to affect the rate of transcription of a number of genes (25). In agreement with this, we observed a drop in the levels of polη mRNA to around 30–50% of the original levels within 6 h of incubation with roscovitine, as monitored by qPCR (Figure 7A). The protein levels of polη appeared to be affected even more, as the roscovitine treatment resulted in a 70% reduction after 3 h and more than a 90% decrease after 6 h (lane 2 and 5 respectively of Figure 7B). The substantial decrease of polη at 6 h indicated that the reduction in protein levels could not be explained only by a block of transcription. To test if protein degradation was involved in this process we combined the treatment with roscovitine with the proteasome inhibitor MG132. The concurrent incubation of MG132 and roscovitine led to a rescue of this phenomenon (compare lanes 4 and 7 with lane 1 Figure 7B) and we could

observe a stabilization of polη, resulting in a 7-fold increase at 6 h, even when its phosphorylation was blocked (compare lanes 5 with lane 7 Figure 7B). During these experiments we did not observe a significant difference in the cell cycle distribution, so we could exclude the possibility that the effects we detected resulted from the cells accumulating in different phases of the cell cycle upon drug treatments (Supplementary Figure S4A).

During our studies we also found that the stable cell line carrying the S687A allele of polη expressed the transgene reproducibly at a lower level (approximately at 30% of WT) than the matching control (Figure 7C, lane 1 and 5). This was a feature that we observed in multiple independent clones (data not shown) even after cell sorting, suggesting that it was not due to the chromosomal locus where the transgene was integrated. This observation was again consistent with a possible role of the phosphorylation of S687 in controlling the polymerase stability. We reasoned that if that were the case, blocking the proteasome with MG132 should restore the protein levels of the S687A mutant to the levels of the WT, possibly with a faster accumulation kinetic after addition of the drug. As can be seen in Figure 7C, exposure to MG132 for just 1 h resulted in doubling the levels of the S687A mutant (compare lane 5 and 6) while very little effect was detected for the WT control (lane 1 and 2). After 6 h of proteasome inhibition, the mutant protein reached the same protein level as its matched control (compare lane 4 and 8).

These two pieces of experimental evidence point to an important role for the phosphorylation in controlling polη stability. We also showed that the polη protein fluctuates during a cell cycle (Figure 5B), increasing toward late S and G2/M phases, matching the pattern of appearance of S687 phosphorylation. If the increase in polη stability was due to the establishment of phosphorylation, we predicted that the S687A protein level would not change during a cell cycle. To test this hypothesis we synchronized the cells in early S phase by double thymidine block before releasing them. Again, the WT showed an increase of polη in S and G2/M before dropping in the G1 of the next cell cycle. Consistent with our hypothesis the S687A mutant showed (i) lower overall protein levels; (ii) hardly any fluctuation in polη during the cell cycle (Figure 7D and E). We conclude that phosphorylation of S687 is important for the regulation of polη protein stability throughout the cell cycle.

DISCUSSION

DNA polymerase η protects the genome by allowing the completion of replication during stress conditions and can bypass CPDs in an error-free manner. Regardless of this characteristic, polη is potentially an error prone polymerase and, along with the other TLS polymerases, it has to be correctly regulated. In yeast, part of the control of TLS is achieved by transcriptional regulation and protein stability (26,27). In human cells, the current working model is that TLS polymerases are controlled by modulating their access to the replication fork by protein–protein interactions and by PTMs. In the case of polη, the protein levels have been reported to be constant throughout the cell cycle (28).
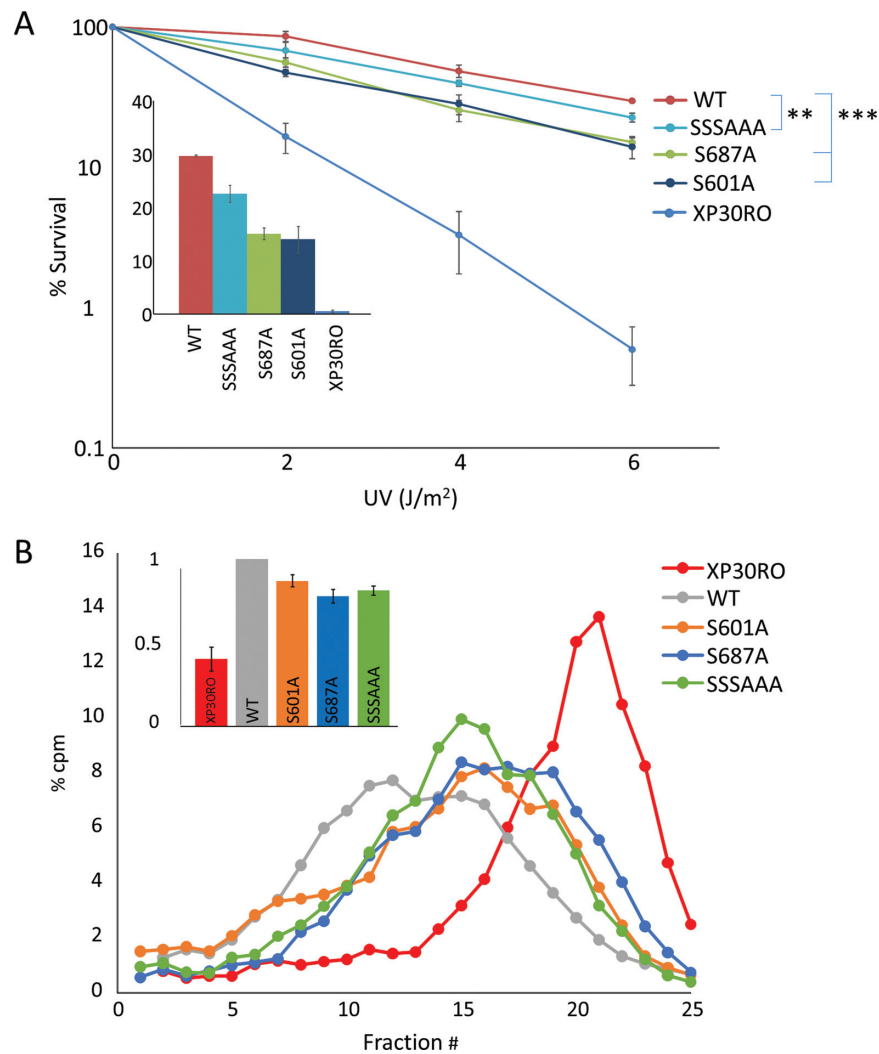
Figure 6. S687 is important for damage bypass and cell survival after UV. (**A**) Clonogenic survival of XP30RO cells expressing various mutant alleles of polη ($n > 3 \pm$ S.E.M). Statistical significance was assessed by t-test: **P = 0.0031, ***P < 0.0001. The inset shows the survival of the cell lines at 6 J/m^2 on a linear scale. (**B**) Damage bypass assay using alkaline sucrose gradient fractionation of newly-synthesized DNA. The inset shows the normalized average molecular weight of DNA from the distributions ($n = 3 \pm$ S.E.M).

Here we show that polη is phosphorylated by CDK2 during an unperturbed cell cycle, with a peak in G2/M and this phosphorylation is important for regulating its stability and activity. We further identify the sites where this modification occurs and demonstrate that missense mutations at these sites affect TLS.

The identification of phosphorylation during an unperturbed cell cycle complements our previous observation that polη was phosphorylated on serine 601 after DNA damage (5). These lines of evidence suggests that phosphorylation plays an even more important role in the framework of TLS regulation. It is interesting to note that Polλ is phosphorylated in a similar manner and its phosphorylation on multiple sites by CDK2 protects it from ubiquitin mediated protein degradation in late S and G2 (29).

Increasing the levels of polη during S phase, with a peak after the bulk of DNA replication is completed provides an appealing form of control to avoid excessive recruitment of a potentially inaccurate polymerase during replication (Fig-ure 8). On the other hand, once the bulk of DNA replication finishes and any remaining gaps in the DNA become a threat to cell survival, increasing the amount of polη would improve the cell's ability to bypass the damaged bases and complete DNA replication. In this situation the presence of polη provides a crucial viability advantage even if the polymerase is inaccurate and could generate mutations in the genome. This model of action is in agreement with observations in yeast and mammalian cells, which showed that TLS was able to function also in late G2 and was not limited to the replicating phase (28,30).

The demonstration that cell-cycle phosphorylation of polη peaks in G2/M suggests a molecular mechanism for this kind of regulation. Interestingly Rev1, another TLS polymerase, has also been found to accumulate in G2 in *S. cerevisiae* (26).

Recently Dai *et al.* identified the phosphorylation of Serine 687 of polη by immunoprecipitating Flag-tagged polη followed by MS (11). They detected a time-dependent in-
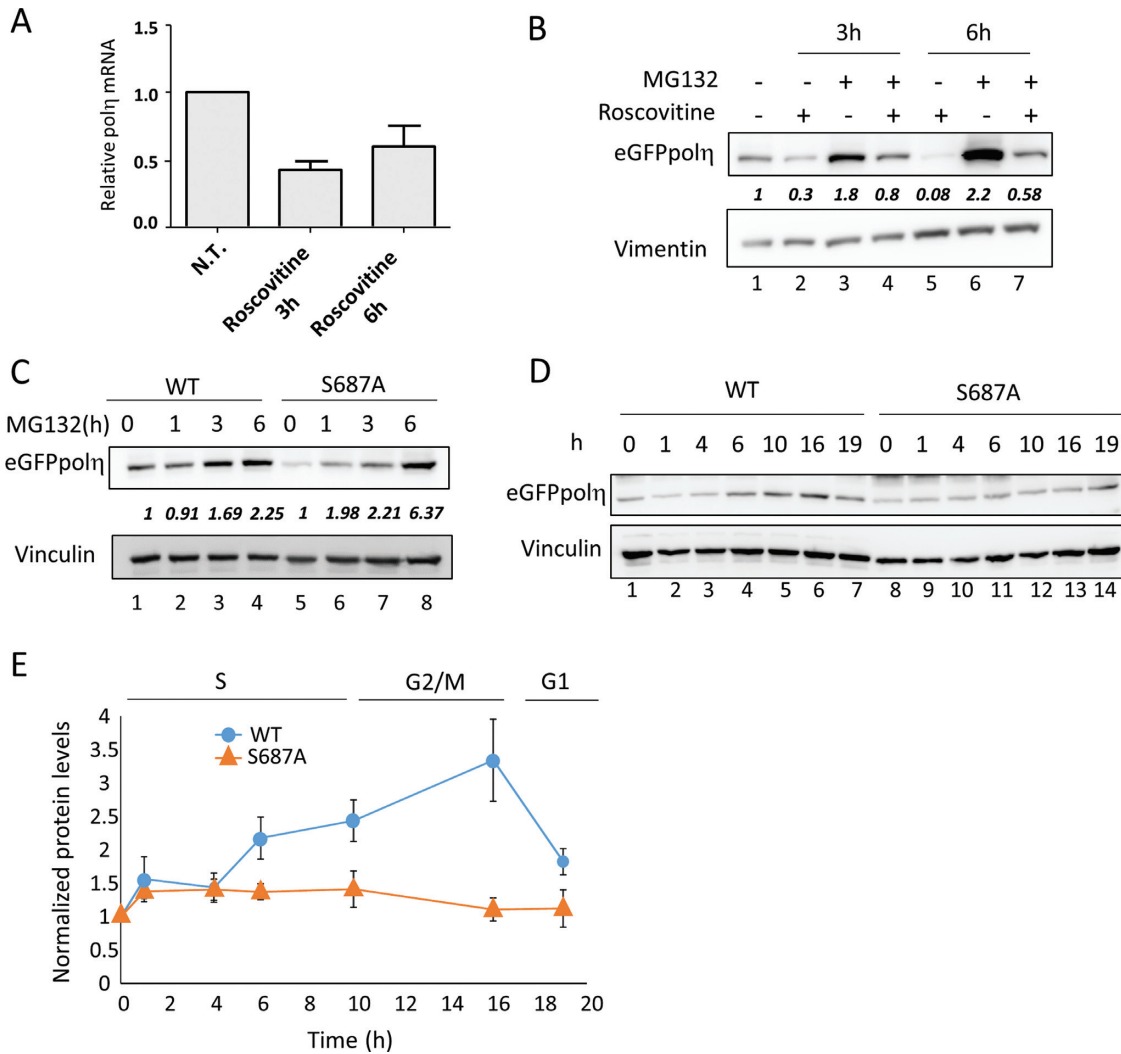
Figure 7. Phosphorylation of polη is important for its stability. (**A**) Transcript levels of polη after CDK inhibition. (**B**) Polη protein levels after roscovitine treatment, in the presence of MG132. Relative protein levels normalized to the untreated sample are displayed in red under the eGFPpolη blot. (**C**) XP30RO cells expressing eGFPpolη WT or S687A were incubated with MG132. Relative protein levels normalized to the 0 h sample of each allele are displayed in bold italic under the eGFPpolη blot. (**D**) XP30RO cells expressing eGFPpolη WT or S687A were synchronized by double thymidine block and followed in the cell cycle after release in nocodazole for 16 h, before final removal of the drug for 3 h. (**E**) Densitometric analysis of polη levels, either WT or S687A, during the cell cycle (mean of three experiments ± S.E.M).

crease in P-S687 after UV irradiation and they speculated that P-S687 mediated the release of the polymerase from PCNA after damage bypass was completed. This model originated from the observation that a C-terminal fragment of polη carrying a S687D mutation had lower affinity for PCNA *in vitro*. By using a phospho-specific antibody we have shown instead that P-S687 decreases over time after UV (Figure 5). One possible explanation for this discrepancy lies in the fact that Dai *et al.* used nocodazole in some of their experiments after UV irradiation, thus increasing the percentage of cells in G2/M. As we have shown, in G2/M the phosphorylation of S687 increases substantially in an unperturbed cell cycle so the compounded effect of UV and nocodazole treatments may have masked the decrease we have observed and resulted in a net apparent increase of P-S687. Furthermore, we failed to observe any difference in binding to PCNA *in vitro* between full length polη

and polη phosphorylated on S687 (Supplementary Figure S3B). Both studies suggest that CDK2 is involved in polη phosphorylation and that S687 could be important for ending TLS activity after damage is bypassed.

The C-terminus of polη contains a number of important regulatory domains such as the NLS (aa 682–694), the UBZ (aa 633–654) and the PIP (aa 701–708). Furthermore, following DNA damage polη is phosphorylated on S601 by ATR. Serine 687 is located in the region that is also referred to as PIR that spans from the canonical PIP to the NLS and contains four lysines that can be ubiquitylated in the absence of DNA damage (4). We confirmed that the S687A mutation did not impair the correct localization of the polymerase (data not shown) and polη appears to be ubiquitylated normally (see Supplementary Figure S2C). Our analysis of P-S687 enables us also to propose that S687 is likely phosphorylated on the diffusing fraction of the polymerase,
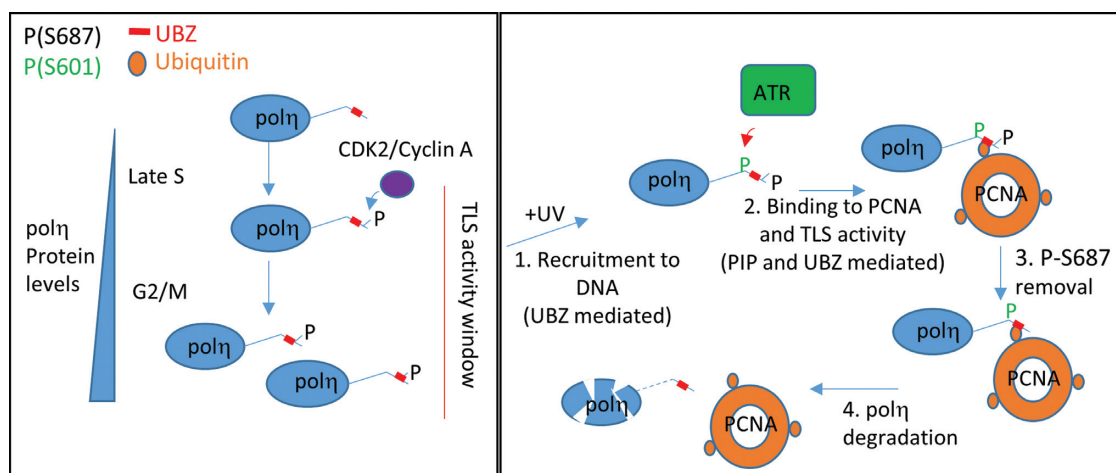
Figure 8. Proposed model of phosphorylation-controlled TLS. During an unperturbed cell cycle polη becomes phosphorylated by CDK2 on Serine 687 from late S to G2/M. This results in the accumulation of the polymerase, which is available for bypass activity (left panel). After damage, phosphorylated polη is recruited to the chromatin via its UBZ (1) and it is further phosphorylated on S601 by ATR. Once S601 has been phosphorylated, polη can interact with Ubiquitylated PCNA and perform TLS (2). Once the damage has been bypassed P-S687 is removed (3) leading to polη degradation (4).

for two reasons: (i) phosphorylation occurs in the absence of DNA damage when the majority of polη is not associated with DNA. (ii) The phosphorylation is not altered in the UBZ mutant (not shown) where polη recruitment to the chromatin is severely hindered. Both in *C. elegans* and mammalian cells, polη appears to be degraded after UV (8) in order to keep the TLS polymerase engaged at a minimum. In *C. elegans*, SUMOylation of polη protects it from degradation by CUL4/Cdt2 and it is removed after damage bypass, leading to removal of the polymerase. In human cells, SUMOylation of polη has been recently identified but with a completely different function (9). Our data suggest that phosphorylation could play a role similar to SUMOylation in *C. elegans*, as S687 defective alleles show enhanced degradation. Furthermore after UV, P-S687 is removed with kinetics similar to that of polη degradation. Serine 687 thus provides an appealing candidate to play the role of regulator of polη, making the polymerase available during the cell cycle and protecting it in the first few hours after DNA damage. In these first crucial moments, polη, stabilized by the phosphorylation of S687, is recruited to DNA via its UBZ. Once on the chromatin, ATR can phosphorylate S601 on polη and the polymerase can interact with ubiquitylated PCNA becoming proficient for damage bypass. Once TLS has been completed P-S687 is removed and this in turn leads to a decrease in polη that could favor resumption of normal replication (Figure 8). How the phosphorylation regulates degradation is an open question.

In recent years, several lines of evidence suggest that polη is important for the bypass of difficult to replicate templates, such as common fragile sites (CFS), even in the absence of damage (31,32). CFS are replicated in late S phase and a large percentage are still unreplicated as the cell enters G2 (33,34). The replication timing of CFS strikingly matches the accumulation of polη and it is tempting to speculate that the accumulation we observe of the polymerase in G2/M could be linked with its CFS bypass role.

It is also interesting to note that damage bypass is impaired *in vivo* in the phosphorylation mutants, although

their catalytic activity is unaffected *in vitro*. As all the functional assays were performed after cell sorting, we can exclude the possibility that the phenotype is merely dependent on reduced protein levels, as the cells expressed the different alleles at similar levels right after sorting, comparable to endogenous polη in MRC5 cells (Supplementary Figure S4B).

Our results complement a recent finding that unveiled how the C-terminus of polη was important for protein stability, by analyzing a mutant allele derived from an XPV patient (10,35). One of the mutations present in XP872VI was a T692A transversion in addition to a STOP codon loss that resulted in a protein with eight extra aminoacids (35). Threonine 692 is located just outside the CDK2 consensus and still in the polη NLS. It is plausible that part of the enhanced degradation of the allele resulted from its defective phosphorylation, further supporting the physiological importance of serine 687 and phosphorylation in general in controlling TLS.

SUPPLEMENTARY DATA

Supplementary Data are available at NAR Online.

ACKNOWLEDGEMENTS

FUNDING

REFERENCES

1. Lehmann,A.R., Niimi,A., Ogi,T., Brown,S., Sabbioneda,S., Wing,J.F., Kannouche,P.L. and Green,C.M. (2007) Translesion synthesis: Y-family polymerases and the polymerase switch. *DNA Repair (Amst)*, **6**, 891–899.
2. Biertumpfel,C., Zhao,Y., Kondo,Y., Ramon-Maiques,S., Gregory,M., Lee,J.Y., Masutani,C., Lehmann,A.R., Hanaoka,F. and Yang,W. (2010) Structure and mechanism of human DNA polymerase eta. *Nature*, **465**, 1044–1048.
3. Sale,J.E., Lehmann,A.R. and Woodgate,R. (2012) Y-family DNA polymerases and their role in tolerance of cellular DNA damage. *Nat. Rev. Mol. Cell Biol.*, **13**, 141–152.
4. Bienko,M., Green,C.M., Sabbioneda,S., Crosetto,N., Matic,I., Hibbert,R.G., Begovic,T., Niimi,A., Mann,M., Lehmann,A.R. *et al.* (2010) Regulation of translesion synthesis DNA polymerase eta by monoubiquitination. *Mol. Cell*, **37**, 396–407.
5. Gohler,T., Sabbioneda,S., Green,C.M. and Lehmann,A.R. (2011) ATR-mediated phosphorylation of DNA polymerase eta is needed for efficient recovery from UV damage. *J. Cell Biol.*, **192**, 219–227.
6. Sabbioneda,S., Bortolomai,I., Giannattasio,M., Plevani,P. and Muzi-Falconi,M. (2007) Yeast Rev1 is cell cycle regulated, phosphorylated in response to DNA damage and its binding to chromosomes is dependent upon MEC1. *DNA Repair (Amst)*, **6**, 121–127.
7. Sabbioneda,S., Green,C.M., Bienko,M., Kannouche,P., Dikic,I. and Lehmann,A.R. (2009) Ubiquitin-binding motif of human DNA polymerase eta is required for correct localization. *Proc. Natl. Acad. Sci. U.S.A.*, **106**, E20.
8. Kim,S.H. and Michael,W.M. (2008) Regulated proteolysis of DNA polymerase eta during the DNA-damage response in C. elegans. *Mol. Cell*, **32**, 757–766.
9. Despras,E., Sittewelle,M., Pouvelle,C., Delrieu,N., Cordonnier,A.M. and Kannouche,P.L. (2016) Rad18-dependent SUMOylation of human specialized DNA polymerase eta is required to prevent under-replicated DNA. *Nat. Commun.*, **7**, 13326.
10. Opletalova,K., Bourillon,A., Yang,W., Pouvelle,C., Armier,J., Despras,E., Ludovic,M., Mateus,C., Robert,C., Kannouche,P. *et al.* (2014) Correlation of phenotype/genotype in a cohort of 23 xeroderma pigmentosum-variant patients reveals 12 new disease-causing POLH mutations. *Hum. Mutat.*, **35**, 117–128.
11. Dai,X., You,C. and Wang,Y. (2016) The functions of serine 687 phosphorylation of human DNA polymerase eta in UV damage tolerance. *Mol. Cell Proteomics*, **15**, 1913–1920.
12. Chen,Y.W., Cleaver,J.E., Hatahet,Z., Honkanen,R.E., Chang,J.Y., Yen,Y. and Chou,K.M. (2008) Human DNA polymerase eta activity and translocation is regulated by phosphorylation. *Proc. Natl. Acad. Sci. U.S.A.*, **105**, 16578–16583.
13. Jung,Y.S., Hakem,A., Hakem,R. and Chen,X. (2011) Pirh2 E3 ubiquitin ligase monoubiquitinates DNA polymerase eta to suppress translesion DNA synthesis. *Mol. Cell. Biol.*, **31**, 3997–4006.
14. Jung,Y.S., Liu,G. and Chen,X. (2010) Pirh2 E3 ubiquitin ligase targets DNA polymerase eta for 20S proteasomal degradation. *Mol. Cell. Biol.*, **30**, 1041–1048.
15. Jung,Y.S., Qian,Y. and Chen,X. (2012) DNA polymerase eta is targeted by Mdm2 for polyubiquitination and proteasomal degradation in response to ultraviolet irradiation. *DNA Repair (Amst)*, **11**, 177–184.
16. Cleaver,J.E., Afzal,V., Feeney,L., McDowell,M., Sadinski,W., Volpe,J.P., Busch,D.B., Coleman,D.M., Ziffer,D.W., Yu,Y. *et al.* (1999) Increased ultraviolet sensitivity and chromosomal instability related to P53 function in the xeroderma pigmentosum variant. *Cancer Res.*, **59**, 1102–1108.
17. Sabbioneda,S., Gourdin,A.M., Green,C.M., Zotter,A., Giglia-Mari,G., Houtsmuller,A., Vermeulen,W. and Lehmann,A.R. (2008) Effect of proliferating cell nuclear antigen ubiquitination and chromatin structure on the dynamic properties of the Y-family DNA polymerases. *Mol. Biol. Cell*, **19**, 5193–5202.
18. Lehmann,A.R. (1972) Postreplication repair of DNA in ultraviolet-irradiated mammalian cells. *J. Mol. Biol.*, **66**, 319–337.
19. Hoffman,P.D., Curtis,M.J., Iwai,S. and Hays,J.B. (2008) Biochemical evolution of DNA polymerase eta: properties of plant, human, and yeast proteins. *Biochemistry*, **47**, 4583–4596.
20. Liang,C.C., Zhan,B., Yoshikawa,Y., Haas,W., Gygi,S.P. and Cohn,M.A. (2015) UHRF1 is a sensor for DNA interstrand crosslinks and recruits FANCD2 to initiate the Fanconi anemia pathway. *Cell Rep.*, **10**, 1947–1956.
21. Parry,D., Guzi,T., Shanahan,F., Davis,N., Prabhavalkar,D., Wiswell,D., Seghezzi,W., Paruch,K., Dwyer,M.P., Doll,R. *et al.* (2010) Dinaciclib (SCH 727965), a novel and potent cyclin-dependent kinase inhibitor. *Mol. Cancer Ther.*, **9**, 2344–2353.
22. De Azevedo,W.F., Leclerc,S., Meijer,L., Havlicek,L., Strnad,M. and Kim,S.H. (1997) Inhibition of cyclin-dependent kinases by purine analogues: crystal structure of human cdk2 complexed with roscovitine. *Eur. J. Biochem.*, **243**, 518–526.
23. Kannouche,P., Broughton,B.C., Volker,M., Hanaoka,F., Mullenders,L.H. and Lehmann,A.R. (2001) Domain structure, localization, and function of DNA polymerase eta, defective in xeroderma pigmentosum variant cells. *Genes Dev.*, **15**, 158–172.
24. Cheng,Q., Cross,B., Li,B., Chen,L., Li,Z. and Chen,J. (2011) Regulation of MDM2 E3 ligase activity by phosphorylation after DNA damage. *Mol. Cell. Biol.*, **31**, 4951–4963.
25. MacCallum,D.E., Melville,J., Frame,S., Watt,K., Anderson,S., Gianella-Borradori,A., Lane,D.P. and Green,S.R. (2005) Seliciclib (CYC202, R-roscovitine) induces cell death in multiple myeloma cells by inhibition of RNA polymerase II-dependent transcription and down-regulation of Mcl-1. *Cancer Res.*, **65**, 5399–5407.
26. Waters,L.S. and Walker,G.C. (2006) The critical mutagenic translesion DNA polymerase Rev1 is highly expressed during G(2)/M phase rather than S phase. *Proc. Natl. Acad. Sci. U.S.A.*, **103**, 8971–8976.
27. Plachta,M., Halas,A., McIntyre,J. and Sledziewska-Gojska,E. (2015) The steady-state level and stability of TLS polymerase eta are cell cycle dependent in the yeast S. cerevisiae. *DNA Repair (Amst)*, **29**, 147–153.
28. Diamant,N., Hendel,A., Vered,I., Carell,T., Reissner,T., de Wind,N., Geacinov,N. and Livneh,Z. (2012) DNA damage bypass operates in the S and G2 phases of the cell cycle and exhibits differential mutagenicity. *Nucleic Acids Res.*, **40**, 170–180.
29. Frouin,I., Toueille,M., Ferrari,E., Shevelev,I. and Hubscher,U. (2005) Phosphorylation of human DNA polymerase lambda by the cyclin-dependent kinase Cdk2/cyclin A complex is modulated by its association with proliferating cell nuclear antigen. *Nucleic Acids Res.*, **33**, 5354–5361.
30. Daigaku,Y., Davies,A.A. and Ulrich,H.D. (2010) Ubiquitin-dependent DNA damage bypass is separable from genome replication. *Nature*, **465**, 951–955.
31. Rey,L., Sidorova,J.M., Puget,N., Boudsocq,F., Biard,D.S., Monnat,R.J Jr, Cazaux,C. and Hoffmann,J.S. (2009) Human DNA polymerase eta is required for common fragile site stability during unperturbed DNA replication. *Mol. Cell. Biol.*, **29**, 3344–3354.
32. Bergoglio,V., Boyer,A.S., Walsh,E., Naim,V., Legube,G., Lee,M.Y., Rey,L., Rosselli,F., Cazaux,C., Eckert,K.A. *et al.* (2013) DNA synthesis by Pol eta promotes fragile site stability by preventing under-replicated DNA in mitosis. *J. Cell Biol.*, **201**, 395–408.
33. Pelliccia,F., Bosco,N., Curatolo,A. and Rocchi,A. (2008) Replication timing of two human common fragile sites: FRA1H and FRA2G. *Cytogenet. Genome Res.*, **121**, 196–200.
34. Palakodeti,A., Han,Y., Jiang,Y. and Le Beau,M.M. (2004) The role of late/slow replication of the FRA16D in common fragile site induction. *Genes Chromosomes Cancer*, **39**, 71–76.
35. Ahmed-Seghir,S., Pouvelle,C., Despras,E., Cordonnier,A., Sarasin,A. and Kannouche,P.L. (2015) Aberrant C-terminal domain of polymerase eta targets the functional enzyme to the proteosomal degradation pathway. *DNA Repair (Amst)*, **29**, 154–165.